

Supplementary Information for:

Choline and lactic acid covalently incorporate into the lignin structure during deep eutectic solvent pulping

Gijs van Erven^{a,b*}, Vincent J. P. Boerkamp^b, Johan W. van Groenestijn^a, Richard J. A. Gosselink^a

^aWageningen Food and Biobased Research, Bornse Weilanden 9, 6708 WG, Wageningen, The Netherlands

^bWageningen University & Research, Laboratory of Food Chemistry, Bornse Weilanden 9, 6708 WG, Wageningen, The Netherlands.

*Corresponding author. Tel: +31 317 487010. E-mail address: gijs.vanerven@wur.nl

Number of pages: 33

Number of tables: 8

Number of figures: 16

Supplementary Information contents:

Experimental details

Table S1. Small scale DES pulping treatments of *Miscanthus* biomass at varying water content and duration.

Table S2. Chemical composition of *Miscanthus*, *Eucalyptus* and pine feedstocks.

Table S3. Chemical composition and recovery of *Miscanthus* R2, residue R6 and lignin R9.

Table S4. Hydroxyl group content of *Miscanthus* native lignin and DES lignin R9 determined by ^{31}P NMR after phosphitylation.

Table S5. ^{13}C -IS pyrolysis-GC-MS relative abundance of lignin derived pyrolysis products in *Miscanthus* feedstock, enzyme lignin and DES fractions.

Table S6. UHPLC-HR-MS annotation of GBG, SBG and VBG reaction products upon DES treatment.

Table S7. Semi-quantitative HSQC NMR structural characterisation of *Miscanthus* DES lignin (R9) fractions following sequential solvent fractionation.

Table S8. Semi-quantitative HSQC NMR structural characterisation of *Miscanthus*, *Eucalyptus* and pine DES lignins obtained at three pulping temperatures.

Figure S1. DES fractionation scheme of *Miscanthus* biomass. R: insoluble residue, S: soluble fraction.

Figure S2. Enzymatic carbohydrate conversion of untreated *Miscanthus* (R2) and the pulp residue following DES pulping (R6) (A) and after mild saponification (B).

Figure S3. Alkaline SEC elution profiles of *Miscanthus* lignin fractions (A) and molecular weight distributions based on total elution profiles and excluding the saponifiable fraction (B).

Figure S4. Selected regions of HSQC spectra of native *Miscanthus* lignin, DES lignin R9 and DES lignin S10 and annotated diketone substructure.

Figure S5. UHPLC-PDA-HR-MS chromatograms of GBG (A) and VBG (B) before and after DES pulping, annotated substructures (C) and semi-quantification based on $\text{UV}_{280\text{nm}}$ absorbance (D, E).

Figure S6. Overlay of aliphatic and aromatic regions of HSQC spectra (400 MHz, DMSO-d_6) of the GBG (A, C) and SBG (B, D) before (black) and after (orange) DES reaction.

Figure S7. Overlay of HSQC spectra of GBG DES with choline chloride (A) and lactic acid, before and after heating at 105°C (B).

Figure S8. Overlay of HSQC (black) and HMBC (orange) spectra of GBG DES (600 MHz, DMSO-d_6) (A) and annotated α -esterified lactic acid substructure (B).

Figure S9. Selected regions of HSQC (A) and HMBC (B) spectra of GBG DES (600 MHz, DMSO-d_6) and annotation of γ -esterified lactic acid substructure (C).

Figure S10. Two-dimensional NMR analysis (600 MHz, DMSO-d_6) of GBG after DES reaction. HMBC (A) and annotated benzylic lactate etherified GBG structure (B).

Figure S11. Two-dimensional NMR analysis (600 MHz, DMSO-d_6) of GBG after DES reaction. HMBC (A), HSQC-TOCSY (B) and annotated benzylic choline etherified GBG structure (C).

Figure S12. Overlay of selected regions of HSQC NMR spectra (600 MHz, DMSO-d_6) of SBG after DES conversion (orange) and DES Lignin R9 before (black in A) and after saponification (black in B, C, D).

Figure S13. HSQC-TOCSY NMR spectra (600 MHz, DMSO-d_6) of DES Lignin R9 before (A) and after saponification (B). Annotated β -5 (blue) and β -5 γ -LA (orange) substructures in C.

Figure S14. Alkaline SEC elution profiles of *Miscanthus* DES lignin fractions following sequential solvent fractionation (A) and molecular weight distributions based on total elution profiles and excluding the saponifiable fraction (B).

Figure S15. Small scale DES pulping lignin precipitate yields and interunit linkage content (HSQC NMR) for *Miscanthus*, *Eucalyptus* and pine feedstocks at increasing pulping temperature.

Figure S16. Small scale DES pulping lignin precipitate yields and structural features as determined by HSQC NMR for various DES water contents and reaction durations.

Experimental details

Materials. *Miscanthus x giganteus* (Cradle Crops, Westdorpe, The Netherlands) was chopped in 5-10 cm long pieces and sequentially milled to pass through a 4 mm and 0.25 mm sieve by using a Wanner C17.26 cutting mill (Wanner Technik GmbH, Wertheim, Germany). Extractive-free *Miscanthus* feedstock was prepared from the milled material (200 g) by sequential Soxhlet solvent extraction using 2 L of water, ethanol and acetone followed by air drying at room temperature. Debarked *Pinus sylvestris* (Staatsbosbeheer, Amersfoort, The Netherlands) and *Eucalyptus grandis* (Klabin, Sao Paulo, Brazil) biomass was chopped to 4 cm chips and milled using the same settings as used for *Miscanthus* and subsequently dried at 40 °C.

Deep eutectic solvent pulping. Lactic acid:choline chloride (10:1 molar ratio), hereafter referred to as DES, was prepared by adding choline chloride to lactic acid under magnetic stirring and gentle heating at 60 °C until a clear solution appeared, and stored in a desiccator until use. Extractive-free *Miscanthus* feedstock (R2, 20 g) was mixed with 400 g DES solution in a 400 mL stainless steel reactor vessel and treated in a 4560 Parr reactor, connected to a 4848 reactor controller (Parr Instrument Company, Moline, IL, USA). Pulping was performed at 120 °C under continuous stirring at 500 rpm for 6 h. After the reaction was completed, the reactor vessel was quenched in cold water under continuous stirring until the temperature reached 60 °C. The material was subsequently transferred to a headspace pressure membrane filtration system to separate the residue from the dark liquor, using a 40 µm pore size polypropylene membrane (Sefar AG, Thal, Switzerland) and max. 2 bar air pressure. The residue on the filter was washed once with 150 g fresh DES and the filtrate was combined with the dark liquor. Residual DES was removed by washing the residue twice with 300 mL 10% v/v ethanol (EtOH) in water. Lignin was precipitated from the dark liquor by dropwise addition to 5 L antisolvent (10% v/v EtOH in water) under vigorous stirring and left to precipitate at room temperature overnight. The formed precipitate was separated through membrane filtration by employing a 1 µm pore size nylon membrane (Sefar AG, Thal, Switzerland) and max. 2 bar air pressure. The precipitate on the filter was washed twice with 300 mL 10% v/v EtOH in water. Both the residue and precipitate were oven-dried at 40 °C. The entire fractionation procedure is presented in Figure S1.

Solid-phase extraction lignin precipitate filtrate. Solid-phase extraction (SPE) was used to isolate the lignin-derived fraction from the precipitation filtrate (S8, Figure S1). A 2g Waters SepPak C18 SPE cartridge (Waters, Milford, MA, USA) was activated with 25 mL methanol (MeOH), equilibrated with 30 mL water and loaded with 90 mL of filtrate (S8) to form a

strongly coloured band on the column. The column was subsequently washed with 50 mL water and eluted with 20 mL MeOH. The eluate was dried under a stream of nitrogen overnight and further oven dried at 40 °C to yield fraction S10 (Figure S1).

Enzymatic lignin isolation from *Miscanthus* and DES cellulose residue. Extractive-free *Miscanthus* (R2, 2 g) and DES cellulose residue (R6, 1 g) were planetary ball-milled in a PM100 planetary ball mill (Retsch, Haan, Germany) with a net milling time of 4 h as previously described.¹ Finely milled materials (1 g) were dispersed in 40 mL 50 mM sodium acetate buffer pH 5, dosed with 30 mg Cellulysin (Sigma-Aldrich, St. Louis, MO, USA) and 125 µL Viscostar 150 L (Dyadic, Jupiter, FL, USA) and incubated for 48 h at 40 °C under rotary shaking at 20 rpm, based on previously published procedures.^{2, 3} The residues were obtained through centrifugation (4,700 x g, 5 min, 20 °C), washed three times with 20 mL water and freeze-dried to respectively yield ‘native lignin’ and residual lignin R11 (Figure S1).

Saponification *Miscanthus*, residue, lignin precipitate and solubilized lignin. Extractive-free *Miscanthus* (R2), DES cellulose residue (R6) and DES lignin (R9) were saponified by dispersing 60 mg material in 3 mL 1 M sodium hydroxide (NaOH) and head-over-tail rotation (30 rpm) for 2 h at room temperature. Samples were acidified to pH 2 with 6 M hydrochloric acid (HCl), centrifuged (2500xg, 20 °C, 2 min) and supernatants were 20 times diluted prior to the quantification of acetic acid and lactic acid as described below. The precipitated saponified DES lignin (R9sap) was washed three times with 10 mL MQ acidified to pH 2 and oven dried at 40 °C.

Saponification of water-soluble lignin was performed by adjusting the pH of 1 L of filtrate S8 to pH 12 by addition of concentrated NaOH. After stirring at room temperature for 15 min, concentrated HCl was added to neutralize the fraction. Saponified solubilized lignin was subsequently purified by SPE using a 10g Waters SepPak tC18 SPE cartridge, using 100 mL MeOH for activation, 100 mL water for equilibration, 250 mL water for washing and 50 mL MeOH for elution. The eluate was dried under a stream of nitrogen at 40 °C.

DES lignin sequential solvent fractionation. Precipitated DES lignin (R9) was sequentially solvent extracted by ethyl acetate (EtOAc), EtOH and MeOH. Hereto, 400 mg lignin was dispersed in 10 mL EtOAc and extracted for 1 h at room temperature using head-over-tail shaking at 20 rpm. The soluble phase was obtained by centrifugation (2,500 x g, 2 min, 20 °C) and the insoluble residue was redispersed in 2 mL EtOAc and centrifuged again. Initial and wash supernatants were combined. The residue was subsequently extracted with EtOH and MeOH following the same procedure. The final residue was washed with an additional 10 mL

MeOH. Soluble phases were filtered through 0.45 μm syringe filters. All fractions were dried under nitrogen at 40 $^{\circ}\text{C}$.

Small scale DES pulping. To determine the effect of biomass type on the overall reaction outcome in terms of yield and lignin structure, small scale DES pretreatments were performed on *Miscanthus*, pine, and *Eucalyptus* biomass. Milled feedstocks (500 mg) were added to glass reaction tubes, mixed with 8 mL DES and vortexed thoroughly before addition to a Stuart SBH200D/3 heating block (Cole Palmer, Vernon Hills, IL, USA) at 120, 140 or 160 $^{\circ}\text{C}$ for a total duration of 1 h, with brief vortexing every 10 min. After the treatment, the tubes were cooled on ice, centrifuged (2,500 \times g, 2 min, 20 $^{\circ}\text{C}$) and 4 mL of the supernatant was transferred to 40 mL 10% v/v EtOH in water, vigorously shaken, and left to precipitate at room temperature for 2 h. Formed precipitates were obtained by centrifugation (4,700 \times g, 5 min, 20 $^{\circ}\text{C}$), washed 3x with 20 mL 10% v/v EtOH in water and oven dried at 40 $^{\circ}\text{C}$.

To test the effect of treatment time and DES water content on the overall reaction outcome in terms of yield and lignin structure, twelve small scale reactions were performed with *Miscanthus* biomass (Table 1), where the LA:ChCl molar ratio and temperature were kept constant at 10:1 (molar ratio) and 120 $^{\circ}\text{C}$, respectively.

For experiments 1-3, 100 g of the DES solution as described in the section ‘Deep eutectic solvent pulping’ was dried by rotary film evaporation at 50 $^{\circ}\text{C}$ and 35 mbar pressure for 90 min, after which the temperature was increased to 60 $^{\circ}\text{C}$ and pressure reduced to 20 mbar and drying continued for another 60 min. Water contents of the original and dried DES were determined by coulometric Karl Fischer titration in duplicate. DES for experiments 7-9 and 10-12 (Table 1) was prepared by respectively adding 10 and 20% w/w water to the original DES. Extractive-free *Miscanthus* (500 mg) was added to glass reaction tubes, mixed with 7.5 g DES and vortexed thoroughly before addition to a Stuart SBH200D/3 heating block (Cole Palmer, Vernon Hills, IL, USA) heating block at 120 $^{\circ}\text{C}$. Tubes were vortexed every 20 min. Work-up was similar as described above.

DES treatment lignin model compounds. Guaiacylglycerol- β -guaiacyl ether (GBG) and syringylglycerol- β -guaiacyl ether (SBG) were used as lignin model compounds for respectively understanding the conversion guaiacyl and syringyl substructures during DES pulping. GBG or SBG (25 mg) were hereto mixed with 1 mL DES in glass reaction tubes, thoroughly vortexed for 1 min and incubated at 100 $^{\circ}\text{C}$ for 30 min in a Stuart SBH200D/3 heating block with vortexing every 5 min. After the reaction, the tubes were cooled to room temperature under running tap water and diluted with 10 mL water. Samples were then purified by SPE using 1g Waters SepPak C18 SPE cartridges, using 10 mL MeOH for

activation, 20 mL water for equilibration, 25 mL water for washing and 10 mL MeOH for elution. After taking a 50 μ L sample for LC-MS analysis, MeOH was removed from the eluate under a stream of nitrogen at 40 °C and the remaining aqueous phase was freeze-dried. The freeze-dried material was dissolved in 0.6 mL deuterated dimethylsulfoxide (DMSO- d_6) for NMR analysis.

Guaiacylglycerol- β -guaiacyl ether (GBG) and Veratrylglycerol- β -guaiacyl ether (VBG) were used as lignin model compounds for respectively understanding the conversion of free phenolic and ‘internal’ nonphenolic substructures during DES pulping. GBG or VBG (25 mg) were hereto mixed with 1 mL 10:1 LA:ChCl (molar ratio), thoroughly vortexed for 1 min and incubated at 100 °C for 30 min at 1000 rpm in a thermomixer (Eppendorf, Hamburg, Germany). After the reaction, the tubes were cooled to room temperature under running tap water, transferred to glass reaction tubes and mixed with 1 mL water and 1 mL EtOAc. The solution was thoroughly vortexed and subsequently centrifuged (2,500 x g, 2 min, 20 °C) to separate the biphasic system. The EtOAc upper layer was transferred to a new glass tube and the lower layer was extracted twice again with 1 mL EtOAc. EtOAc fractions were combined and 20 μ L sample was taken and 50x diluted in 50% v/v aqueous MeOH prior to LC-MS analysis.

Enzymatic carbohydrate hydrolysis. Extractive-free *Miscanthus* (R2) and DES cellulose residue (R6) were dispersed at 5 % w/w in 50 mM sodium acetate buffer at pH 5 (2 g/38 mL). Cellic CTec2 was added (200 μ L) to give a total protein dose of 1.25% w/w of the substrate dry matter.⁴ PenStrep (40 μ L) was used to prevent microbial growth. Samples were incubated at 50°C for 72 h with constant head-over-tail rotation at 20 rpm. After incubation, the enzymes were deactivated by heating the samples at 100 °C for 5 min. After cooling down to room temperature, the solid and liquid fractions were separated by centrifugation (4,700 x g, 5 min, 20 °C). The supernatants were analysed for glucose and xylose by HPAEC as published.⁵ Mild saponification of the substrates prior to enzymatic hydrolysis was evaluated by mixing 1 g of respective R2 or R6 material with 5 mL 0.05 M NaOH or 0.2 M NaOH, followed by incubation for 1 h at 50°C. Samples were subsequently acidified to pH 5 with glacial acetic acid and mixed with buffer to reach 5% w/w. CellicCTec2 and Penstrep were added in equal dry matter dosages as above and incubation and work-up was identical as described.

Compositional analysis. Two grams of milled pine and *Eucalyptus* feedstock were sequentially extracted with ethanol/toluene (2:1 v/v), toluene and water in an automated solvent extraction system (Dionex™ ASE™ 350 Accelerated Solvent Extractor) and residues

were subsequently oven dried at 40 °C. Extractive-free pine, *Eucalyptus* and *Miscanthus* (R2), precipitated lignin (R9) and the cellulose residue (R6) (Figure 1) were hydrolyzed in duplicate with 72% (w/w) H₂SO₄ for 1 h at 30 °C followed by 1 M H₂SO₄ for 3 h at 100 °C. The acid insoluble lignin (AIL) was determined gravimetrically after washing the hydrolysis residue until the pH of the filtrate was neutral. AIL was corrected for ash content through thermogravimetric analysis (TGA) until 900 °C under nitrogen atmosphere. Acid soluble lignin in the hydrolysate was determined spectrophotometrically at 205 nm using an extinction coefficient of 110 L g⁻¹ cm⁻¹. Constituent neutral monosaccharides in the hydrolysate were quantified by high-performance anion exchange chromatography with pulsed amperometric detection (HPAEC-PAD) as reported previously and expressed as anhydromonosaccharides.⁵ Uronic acids in the hydrolysate were determined spectrophotometrically according to the method of Blumenkrantz and likewise expressed as anhydro analogs.⁶

Organic acid content. Samples were diluted with water and filtered using a 0.45 µm PFTE filter. A Vanquish UHPLC (Thermo Scientific) equipped with an Aminex-87H column (Biorad) and a refractive index (RI) and ultraviolet (UV) detector at 210 nm detector was used for separation and quantification on the basis of calibration curves for acetic and lactic acid. Elution was performed isocratically with 50 mM sulfuric acid (H₂SO₄) at a flow rate of 0.6 mL min⁻¹ at 55 °C.

Quantitative pyrolysis-GC-MS with ¹³C lignin as internal standard. To quantify lignin content and structural features, lignin fractions were analysed by quantitative pyrolysis-GC-MS. Analytical pyrolysis coupled to gas chromatography with high-resolution mass spectrometric detection (Exacte Orbitrap, Thermo Scientific, Waltham, MA, USA) was performed as previously described, using an Agilent VF-1701ms column (30 m x 0.25 i.d. 0.25 µm film) for chromatographic separation.⁷ Uniformly ¹³C-labeled lignin (97.7 atom% ¹³C), isolated from ¹³C wheat straw (IsoLife BV, Wageningen, The Netherlands) was used as an internal standard (¹³C-IS).⁸ To each accurately weighed sample (80 µg), 10 µL of a ¹³C-IS solution (1 mg·mL⁻¹ ethanol/chloroform 50:50 v/v) was added and dried prior to analysis. All samples were prepared and analysed in duplicate. Lignin-derived pyrolysis products were monitored in full MS mode on the most abundant fragment per compound (both nonlabeled and uniformly ¹³C labelled). Pyrograms were processed by TraceFinder 4.0 software. Lignin contents and relative abundances of lignin-derived pyrolysis products were calculated as described previously.⁷

NMR spectroscopy. Approximately 30 mg of sample was dissolved in 0.6 mL DMSO-d₆ for NMR measurements. Routine ¹H-¹³C HSQC measurements were performed on a Bruker AVANCE III 400 MHz instrument equipped with a 5 mm BBI probe with z-gradient (5 G cm⁻¹ A⁻¹) (Bruker BioSpin, Rheinstetten, Germany). Spectra were recorded by using the adiabatic “hsqcetgpsisp2.2” pulse sequence using the following parameters: spectral width of 4,800 Hz (12 ppm) in F1 (¹H) using 1922 increments for an acquisition time (AQ) of 0.2 s and interscan delay (D1) of 1.0 s and a spectral width of 20,000 Hz (200 ppm) in F2 (¹³C) using 322 increments with an AQ of 8 ms with 32 scans per increment. The ¹J_{CH} used was 145 Hz. Processing used Gaussian apodization (GB = 0.001, LB = -0.2) in the ¹H dimension and a squared cosine function (SSB = 2) in the ¹³C dimension.

For structural elucidation, measurements were performed on a Bruker AVANCE III 600 MHz NMR spectrometer (Bruker BioSpin, Rheinstetten, Germany) equipped with a 5 mm cryo-probe located at MAGNEFY (MAGNEtic resonance research FacilitY, Wageningen, The Netherlands).

¹H-¹³C HSQC spectra were recorded by using the adiabatic “hsqcetgpsisp2.2” pulse sequence using the following parameters: spectral width of 7,200 Hz (12 ppm) in F1 (¹H) using 4096 increments for an acquisition time (AQ) of 0.29 s and interscan delay (D1) of 1.0 s and a spectral width of 33,000 Hz (220 ppm) in F2 (¹³C) using 512 increments with an AQ of 8 ms with 16 scans per increment. The ¹J_{CH} used was 145 Hz.

¹H-¹³C HSQC-TOCSY NMR spectra were recorded by using the “hsqcetgpml” pulse sequence using the following parameters: spectral width of 7,200 Hz (12 ppm) in F1 (¹H) using 2048 increments for an acquisition time (AQ) of 0.14 s and interscan delay (D1) of 1.3 s and a spectral width of 33,000 Hz (220 ppm) in F2 (¹³C) using 512 increments with an AQ of 8 ms with 16 scans per increment. The ¹J_{CH} used was 145 Hz.

¹H-¹³C HMBC NMR spectra were recorded by using the “hmbcgpplndqf” pulse sequence using the following parameters: spectral width of 7,200 Hz (12 ppm) in F1 (¹H) using 4096 increments with an AQ of 0.29 s and D1 of 1.5 s and a spectral width of 33,000 Hz (220 ppm) in F2 (¹³C) using 512 increments with an AQ of 8 ms with 128 scans per increment, using a 76 ms long-range coupling delay (D6). Processing used Gaussian apodization (GB = 0.001, LB = -0.01) in the ¹H dimension and a squared cosine function (SSB = 2) in the ¹³C dimension.

¹³C band selective ¹H-¹³C HSQC spectra were recorded by using the adiabatic “shsqcetgpsisp2.2” pulse sequence using the following parameters: spectral width of 7,200 Hz (12 ppm) in F1 (¹H) using 4096 increments for an acquisition time (AQ) of 0.29 s and

interscan delay (D1) of 1.0 s and a spectral width of 6,800 Hz (45 ppm, from 45 to 90 ppm) in F2 (^{13}C) using 160 increments with an AQ of 12 ms with 32 scans per increment. The $^1J_{\text{CH}}$ used was 145 Hz.

^{13}C band selective ^1H - ^{13}C HMBC spectra were recorded by using the “shmbcctetgp12nd” pulse sequence using the following parameters: spectral width of 7,200 Hz (12 ppm) in F1 (^1H) using 4096 increments with an AQ of 0.29 s and D1 of 1.5 s and a spectral width of 6,800 Hz (45 ppm, from 45 to 90 ppm) in F2 (^{13}C) using 160 increments with an AQ of 12 ms with 32 scans per increment, using a 76 ms long-range coupling delay (D6).

In all spectra, the central solvent peak was used as an internal reference (δ_{C} 39.5 ppm; δ_{H} 2.49 ppm). The spectra were processed using TopSpin 4.0 software.

Semi-quantitative analysis of the HSQC volume integrals was performed according to Del Río et al.,⁹ making use of the chemical shifts reported in the literature for annotation.¹⁰ $\text{S}_{2,6}$, G_2 and $\text{H}_{2,6}$ signals were used for S, G and H units, respectively, where S and H integrals were logically halved. Oxidized analogues were estimated in a similar manner. Tricin, *p*CA and FA were similarly estimated from their respective $\text{T}_{2,6}$, $\text{pCA}_{2,6}$ and FA_2 signals, respectively. $\text{H}_{2,6}$ integrals were corrected for the overlapping phenylalanine cross-peak ($\text{PHE}_{3,5}$) by subtraction of the isolated $\text{PHE}_{2,6}$ cross-peak.¹¹ In the aliphatic oxygenated region β -O-4 aryl ether substructures were estimated from their C_{β} - H_{β} correlations. For β -5 phenylcoumaran, β - β resinol and β - β tetrahydrofuran substructures, their respective C_{α} - H_{α} correlations were used. Volume integrals for β - β resinol and β - β tetrahydrofuran substructures were logically halved. Cinnamyl alcohol and cinnamaldehyde substructures were estimated from their C_{γ} - H_{γ} correlations and volume integrals for the former were halved. Hibbert ketone substructures were estimated from the C_{γ} - H_{γ} correlations and integrals halved as well. Benzaldehyde substructures were estimated from their C_{α} - H_{α} signal. Bound choline was quantified on its C_2 - H_2 (CH_2) correlation peak, because the C_1 - H_1 (CH_1) correlation is severely overlapped by C_{γ} - H_{γ} correlations of β -5 phenylcoumaran substructures and the trimethylammonium ($\text{R-N}^+(\text{CH}_3)_3$) signal does not allow distinguishing free and bound choline, and is overlapped by the C_{β} - H_{β} correlation peak of resinol substructures. Lactic acid was quantified on the basis of the C_2 - H_2 correlation peak at $\delta_{\text{C}}/\delta_{\text{H}}$ 67.9/5.0 ppm, because the 65.5/4.0 ppm correlation peak is severely overlapped by C_{γ} - H_{γ} correlations of acylated β -O-4 units. Etherified lactic acid was quantified on the basis of the C_2 - H_2 correlation peaks at $\delta_{\text{C}}/\delta_{\text{H}}$ 72.7/4.0 ppm and 71.1/3.76, the latter corrected for overlapping C_{γ} - H_{γ} β - β resinol correlations by subtracting the isolated C_{γ} - H_{γ} β - β resinol correlation peak at 71.0/4.15 ppm.

Volume integration of all signals was performed at equal contour levels. Contour levels were normalized at equal size of the $-OCH_3$ integral. Abundance was calculated as a percentage of total lignin ($H + G + G_{ox} + S + S_{ox}$) (per 100 aromatic rings).

^{31}P NMR spectroscopy. ^{31}P NMR was performed as previously described.¹² Around 30 mg of enzyme lignin or DES precipitated lignin (R9) was mixed with 100 μL *N,N*-dimethylformamide (DMF)/pyridine (50:50 v/v) and 100 μL pyridine containing 15 mg mL^{-1} cyclohexanol as internal standard and 2.5 mg mL^{-1} chromium(III) acetylacetonate as relaxation agent and stirred overnight to dissolve. Derivatization of the dissolved lignins was performed by the addition of 2-chloro-4,4,5,5-tetramethyl-1,3,2-dioxaphospholane (100 μL pre-mixed with 400 μL of deuterated chloroform). The phosphitylated lignins were measured on a Bruker AVANCE III 400 MHz instrument using a standard phosphorus pulse sequence with 30° pulse angle (“zgig30”), inverse gated proton decoupling, using 64k increments with an AQ of 0.67 s and D1 of 5 s with 256 scans per increment. Processing used Exponential apodization with LB = 4 Hz). Signals were assigned according to Granata and Agyropoulos (1995) and integrated by using MestReNova 10 software.¹³

Size-exclusion chromatography (SEC). Alkaline SEC was performed as described by Constant et al. (Method D).¹⁴ Briefly, lignin fractions were dissolved in 0.5 M NaOH (eluent) in a concentration of 1 mg mL^{-1} and separated by using two TSKgel GMPWxl columns (7.8 x 300 mm, particle size 13 μm) in series equipped with a TSKgel guardcolumn PWxl (6.0 x 40 mm, particle size 12 μm). Absorption was monitored at 280 nm with an ultraviolet spectroscopy detector. Sodium polystyrene sulphonate (PSS) standards and phenol were used for calibration. Protobind™ 1000 lignin (Wheat straw/Sarkanda grass soda lignin, GreenValue S.A, Switzerland) was used as reference.

UHPLC-PDA-HR-MS. Reaction products of the DES treatment of lignin model compounds were separated by using a Vanquish UHPLC system (Thermo Scientific), equipped with a pump, degasser, autosampler and photodiode array (PDA) detector. Samples were 20x diluted in MeOH for PDA detection and diluted 10x further for accurate mass analysis. Samples (1 μL) were injected onto an Acquity UPLC BEH C18 column (150 x 2.1 mm, particle size 1.7 μm) with VanGuard (5 mm x 2.1 mm, particle size 1.7 μm) (Waters, Milford, MA, USA). The column compartment heater, eluent preheater and post-column cooler were set to 45 °C, 45 °C and 40 °C, respectively. The flow rate was 0.4 $mL\ min^{-1}$. Water (A) and acetonitrile (B), both acidified with 0.1% (v/v) formic acid, were used as eluents. The following gradient was used: 0-1.09 min at 5% B (isocratic), 1.09-26.98 min from 5 to 100% B (linear gradient), 26.98-32.43 min at 100% B (isocratic), 32.43-33.52 min from 100 to 5% B (linear gradient) and

33.52-38.97 min at 5% B (isocratic). The PDA detector was set to record absorbance between 190 and 680 nm. The Vanquish UHPLC system was coupled to a Thermo Q Exactive Focus hybrid quadrupole-orbitrap mass spectrometer (Thermo Scientific) equipped with a heated ESI probe. The mass spectrometer was calibrated by using Tune 2.11 software (Thermo Scientific) by direct infusion of Pierce negative and positive ion LTQ ESI calibration solutions (Thermo Scientific). Full MS data were recorded in positive ionization mode over a range of m/z 200-1,000 at a resolution of 70,000. Higher energy C-trap dissociation (HCD) fragmentation was performed at 35% normalized collision energy and fragments were recorded at 35,000 resolution. MS2 fragmentation was performed on the most abundant ion in full MS with dynamic exclusion enabled and automated by Tune 2.11 software to obtain MS2 spectra of multiple different ions present in the full MS spectra at the same time. Nitrogen was used as sheath gas (50 arbitrary units), auxiliary gas (13 arbitrary units) and sweep gas (1 arbitrary units). The capillary temperature was 263 °C; the probe heater temperature was 425 °C; the source voltage was 3.5 kV; and the S-lens RF level was 50. Data processing was done using Xcalibur 4.5 (Thermo Scientific).

Table S1. Small scale DES pulping treatments of *Miscanthus* biomass at varying water content and duration.

Exp.no	LA:ChCl (molar ratio)	Temperature (°C)	Water content (% w/w)	Time (h)
1	10:1	120	4.4 ± 0.1	6
2				3
3				1
4	10:1	120	13.2 ± 0.3	6
5				3
6				1
7	10:1	120	21.9 ± 0.3	6
8				3
9				1
10	10:1	120	30.5 ± 0.2	6
11				3
12				1

Table S2. Chemical composition of *Miscanthus*, *Eucalyptus* and pine feedstocks.

	Content (% w/w)										
	Extractives	Glucan	Arabinan	Xylan	Mannan	Galactan	Glucuronan	AIL ^a	ASL ^b	Ash	Protein
<i>Miscanthus</i>	5.7	40.7	1.7	17.4	0.1	0.4	0.8	18.6	0.9	3.1	0.6
<i>Eucalyptus</i>	4.0	37.8	0.2	9.0	0.8	0.8	3.9	21.2	1.8	n.d.	n.d.
Pine	4.4	35.6	0.8	3.8	10.8	1.4	3.2	25.0	0.2	n.d.	n.d.

^aAcid-insoluble lignin, corrected for ash; ^bAcid-soluble lignin; n.d. not determined

Table S3. Chemical composition and recovery of *Miscanthus* R2, residue R6 and lignin R9.

	Content (% w/w)					Recovery (% w/w)			
	Cellulose	Hemicellulose ^a	Lignin ^b	Ash	Lactic Acid	Dry matter	Cellulose	Hemicellulose	Lignin
R2 <i>Miscanthus</i>	40.7 ± 0.1	19.8 ± 0.1	19.4 ± 0.6	3.1 ± 0.9	n.d.	-	-	-	-
R6 residue	71.7 ± 1.5	12.7 ± 0.1	5.6 ± 0.0	1.4 ± 0.1	15.6	65	115 ^c	42	19
R9 lignin	3.2 ± 0.0	2.4 ± 0.0	76.3 ± 1.8	1.1 ± 0.1	12.0	13	1	2	51

^a: sum of anhydroarabinose, anhydroxylose and anhydrouronic acid; ^b: sum of AIL corrected for ash and ASL; ^c: this excessive recovery is likely due to the fact that residual cellulose is more completely acid-hydrolyzed than the cellulose in the initial feedstock.

Additional discussion DES lignin and cellulose purity and cellulose valorisation. The relatively low purity of the precipitated lignin (R9, 76.3% w/w) is primarily due to the presence of lactic acid (12.0% w.w), and also due to residual carbohydrates (5.6 % w/w). The cellulose content of the residue (R6) (71.7% w/w) is worth considering for further valorisation incentives. This purity is promising given the relatively mild conditions used compared to traditional soda pulping processes applied to herbaceous feedstocks and even more so because of the substantial amounts of lactic acid present (Table S3). Being esterified, this lactic acid could be an easy target for cellulose purification via mild alkali, thus avoiding intensive bleaching procedures. Additionally, the lignin content of the R6 residue is at a relatively low level and might further decrease upon alkaline purification. Alternatively, the introduction of these lactate esters into the polysaccharide fraction could potentially offer interesting properties for further exploitation. Importantly, the substantial incorporation of lactic acid into the pulp residue (R6) severely impacted the enzymatic conversion, especially that of cellulose

(Figure S2). Despite the extensive delignification (>70%) cellulose digestibility was only marginally improved as compared to untreated miscanthus. Morais et al. have previously demonstrated that DES treatment can result in substantial cellulose esterification¹⁵ and Zeng et al. recently showed that this esterification impairs cellulase hydrolysis.¹⁶ Indeed, subsequent mild alkaline pretreatment to remove these lactate esters could improve cellulose conversion by up to 2.6-fold. Residual xylan conversion was also improved, but to a much lesser extent. This implies that esterification preferentially occurred on cellulose or that xylanases in the enzyme cocktail were affected less. Given the necessity of sequential saponification, we consider material applications of DES cellulose more worthwhile to explore than monosaccharide-oriented valorisation routes.

Table S4. Hydroxyl group content of *Miscanthus* enzyme lignin and DES lignin R9 determined by ^{31}P NMR after phosphitylation.

(mmol/g lignin) ^a	<i>Miscanthus</i> native	DES lignin R9
Aliphatic OH + carb. OH	5.37	4.77
S-OH	0.12	0.49
5-sub. G-OH	0.22	0.56
G-OH	0.45	0.86
H-OH + pCA-OH	0.57	1.09
Total phenolic OH	1.37	3.00
COOH	0.12	0.67

^acontents per g biomass corrected for lignin contents as determined by quantitative ^{13}C -IS py-GC-MS (*Miscanthus* native lignin: 88.4% w/w; DES lignin R9 69.5%w/w)

Table S5. ^{13}C -IS pyrolysis-GC-MS relative abundance of lignin derived pyrolysis products in *Miscanthus* feedstock, enzyme lignin and DES fractions. Corrected for RRF and relative abundance of ^{13}C analogues. Sum on the bases of structural classification according to van Erven et al. (2019, 2023).^{5, 17} Average and standard deviation of analytical duplicates. Codes refer to Figure 1.

	<i>Miscanthus</i> R2	<i>Miscanthus</i> native lignin	DES residue R6	DES lignin R9	DES soluble lignin S10
Lignin subunits (%)					
H	33.7 ± 0.2	30.5 ± 2.4	43.3 ± 0.3	33.0 ± 0.2	14.8 ± 0.2
G	46.5 ± 0.1	45.8 ± 1.2	39.1 ± 0.1	40.8 ± 0.5	61.2 ± 2.5
S	19.9 ± 0.3	23.8 ± 1.3	17.6 ± 0.2	26.3 ± 0.2	24.0 ± 2.7
S/G	0.43 ± 0.0	0.52 ± 0.0	0.45 ± 0.0	0.64 ± 0.0	0.39 ± 0.1
<i>trans</i> -coumaryl Alc.	1.6 ± 0.0	1.8 ± 0.0	1.2 ± 0.0	0.9 ± 0.1	0.7 ± 0.0
<i>trans</i> -coniferyl Alc.	63.3 ± 0.1	62.8 ± 0.5	66.3 ± 0.1	56.7 ± 0.3	62.4 ± 3.7
<i>trans</i> -sinapyl Alc.	35.1 ± 0.2	35.5 ± 0.6	32.6 ± 0.2	42.4 ± 0.4	36.9 ± 3.7
tSinA/tConA	0.55 ± 0.0	0.57 ± 0.0	0.49 ± 0.0	0.75 ± 0.0	0.59 ± 0.1
Structural moieties (%)					
Unsubstituted	5.2 ± 0.1	5.9 ± 0.6	10.0 ± 0.1	11.0 ± 0.2	5.7 ± 0.2
Methyl	2.7 ± 0.0	3.2 ± 0.2	5.5 ± 0.2	4.1 ± 0.0	1.8 ± 0.1
Vinyl	53.4 ± 0.9	44.4 ± 2.9	57.0 ± 0.4	48.2 ± 0.2	42.1 ± 3.8
4-VP ^a	30.6 ± 0.2	27.1 ± 2.3	36.6 ± 0.2	27.7 ± 0.3	12.6 ± 0.3
4-VG ^b	19.7 ± 0.6	14.2 ± 0.6	17.0 ± 0.2	15.4 ± 0.4	27.5 ± 3.6
C α -ox	4.2 ± 0.0	4.1 ± 0.2	5.1 ± 0.1	4.5 ± 0.0	11.3 ± 1.5
diketones	0.4 ± 0.0	0.4 ± 0.0	1.4 ± 0.0	1.2 ± 0.0	7.2 ± 1.2
C β -ox ^c	1.3 ± 0.0	1.2 ± 0.0	2.7 ± 0.1	2.2 ± 0.0	1.5 ± 0.1
C γ -ox	28.4 ± 0.7	36.0 ± 3.7	13.7 ± 0.8	24.4 ± 0.5	35.3 ± 4.8
Miscellaneous	4.7 ± 0.2	5.3 ± 0.3	5.9 ± 0.1	5.6 ± 0.4	2.3 ± 0.1
PhC γ ^d	33.7 ± 0.8	41.6 ± 3.5	21.1 ± 0.7	31.3 ± 0.7	38.4 ± 4.9

^a 4-vinylphenol. ^b 4-vinylguaiacol. ^c excluding diketones. ^d phenols with intact α,β,γ carbon side chain, excluding diketones.

Additional discussion pyrolysis-GC-MS. In line with HSQC NMR analysis, pyrolysis-GC-MS demonstrated that the lignins in the residual, precipitated and solubilized fractions substantially differed in subunit composition, with S/G ratios of 0.45, 0.64 and 0.39, respectively. The more specific 4-hydroxyphenylpropanoid distributions (coumaryl alcohol (tCouA):coniferyl alcohol (tConA): sinapyl alcohol (tSinA)) indicated likewise, with tSinA/tConA ratios of 0.49, 0.75 and 0.59 for the respective fractions. All fractions were decreased in intact interunit linkages as evidenced from a reduced abundance of pyrolysis products with an intact three-carbon side chain (PhC γ). The abundance of 4-vinylphenol suggested that *p*-coumaric acid moieties were largely preserved during DES pulping. Remarkably, though, the soluble fraction (S10) showed a depletion of said moieties, while 4-vinylguaiacol, largely derived from ferulic acid, increased. DES lignin fractions were increased in C α -oxidized substructures, the soluble lignin (S10) in particular. The remarkable increase in diketone pyrolysis products observed in this fraction was caused by both guaiacyl- (4.0%) and syringyl diketones (3.3%). Given the subunit composition, it is clear that syringyl units are more susceptible to conversion towards diketones.

Table S6. UHPLC-HR-MS annotation of GBG, SBG and VBG reaction products upon DES treatment

Retention time MS (min)	Annotation	Molecular formula	Ionization	Observed/calculated mass	Mass error (ppm)	MS ² fragments
4.69	TriLA-Ch	C ₁₄ H ₂₆ O ₇ N	[M ⁺]	320.17056/320.170929	1.15	189.07576, 261.09665
7.00, 7.10	GBG-Ch	C ₂₂ H ₃₂ O ₆ N	[M ⁺]	406.22240/406.22296	1.39	104.10731
7.89, 8.17, 8.23	GBG-Ch-LA	C ₂₅ H ₃₆ O ₈ N	[M ⁺]	478.24364/478.24409	0.95	104.10738, 151.07532, 266.17480
9.20, 9.30	GBG-Ch-diLA	C ₂₈ H ₄₀ O ₁₀ N	[M ⁺]	550.26497/550.26522	0.46	253.08582, 151.07538, 104.10744
8.55, 8.60	GBG	C ₁₇ H ₂₀ O ₆	[M+Na ⁺]	343.11572/343.11576	0.12	146.03394, 175.03662
9.56-9.82	GBG-LA	C ₂₀ H ₂₄ O ₈	[M+Na ⁺]	415.13626/415.13689	1.52	202.05994, 146.03372, 113.02114
9.88	GBG-LA	C ₂₀ H ₂₄ O ₈	[M+Na ⁺]	415.13626/415.13689	1.52	146.03377, 202.05970, 343.11469
10.39, 10.87	GBG-LA	C ₂₀ H ₂₄ O ₈	[M+Na ⁺]	415.13639/415.13689	1.20	202.05994, 149.05969, 137.05971
10.70-11.50	GBG-diLA	C ₂₃ H ₂₈ O ₁₀	[M+Na ⁺]	487.15771/487.158019	0.63	185.05737, 274.08099, 146.03391
11.64	GBG-diLA	C ₂₃ H ₂₈ O ₁₀	[M+Na ⁺]	487.15778/487.158019	0.49	202.05998, 146.03392, 185.04185
11.78	GBG-diLA	C ₂₃ H ₂₈ O ₁₀	[M+Na ⁺]	487.15784/487.158019	0.37	n.d.
12.17	GBG-diLA	C ₂₃ H ₂₈ O ₁₀	[M+Na ⁺]	487.15778/487.158019	0.49	202.06004, 146.03382, 185.04213
11.62-12.70	GBG-triLA	C ₂₆ H ₃₂ O ₁₂	[M+Na ⁺]	559.17908/559.17915	0.13	185.05733, 274.08090, 146.03389
13.37	GBG dimer	C ₃₄ H ₃₈ O ₁₁	[M+Na ⁺]	645.23109/645.23118	0.15	146.03381, 343.11481, 505.18243
6.96	SBG-Ch	C ₂₃ H ₃₄ O ₇ N	[M ⁺]	436.23341/436.23353	0.27	104.10738, 181.08585
7.87	SBG-Ch-LA	C ₂₆ H ₃₈ O ₉ N	[M ⁺]	508.25469/508.25466	0.06	104.10735, 181.08578, 296.18530
8.03	SBG-Ch-LA	C ₂₆ H ₃₈ O ₉ N	[M ⁺]	508.25462/508.25466	0.08	n.d.
8.10	SBG-Ch-LA	C ₂₆ H ₃₈ O ₉ N	[M ⁺]	508.25445/508.25466	0.41	n.d.
9.15	SBG-Ch-diLA	C ₂₉ H ₄₂ O ₁₁ N	[M ⁺]	580.27543/580.27579	0.62	104.10741, 181.08589, 296.18564
8.33, 8.47	SBG	C ₁₈ H ₂₂ O ₇	[M+Na ⁺]	373.12570/373.12632	1.67	146.03389, 205.04709
9.30-10.45	SBG-LA	C ₂₁ H ₂₆ O ₉	[M+NH ₄ ⁺]	440.19196/440.19206	0.22	149.05977, 167.07027, 191.07024
10.39-11.85	SBG-diLA	C ₂₄ H ₃₀ O ₁₁	[M+Na ⁺]	517.16845/517.16858	0.26	215.06779, 304.09149, 283.09628
11.40-12.90	SBG-triLA	C ₂₇ H ₃₄ O ₁₃	[M+Na ⁺]	589.18987/589.18970	0.26	n.d.
12.85	SBG dimer	C ₃₆ H ₄₂ O ₁₃	[M+Na ⁺]	705.25215/705.25231	0.23	159.04158, 146.03377, 373.12537
8.08, 8.24	VBG-Ch	C ₂₃ H ₃₄ O ₆ N	[M ⁺]	420.23789/420.23861	1.63	104.10731, 151.07526, 165.09095
8.86, 9.22	VBG-Ch-LA	C ₂₆ H ₃₈ O ₈ N	[M ⁺]	492.25909/492.25974	1.32	104.10728, 165.09085, 280.19028
9.93	VBG	C ₁₈ H ₂₂ O ₆	[M+NH ₄ ⁺]	352.17528/352.17601	2.02	151.07524, 176.08307, 164.08324
10.71-11.28	VBG-LA	C ₂₁ H ₂₆ O ₈	[M+Na ⁺]	429.15172/429.15254	1.91	149.05966, 176.08316, 151.07532
11.73	VBG-LA	C ₂₁ H ₂₆ O ₈	[M+Na ⁺]	429.15179/429.15254	1.75	n.d.
12.26	VBG-LA	C ₂₁ H ₂₆ O ₈	[M+Na ⁺]	429.15177/429.15254	1.79	149.05962, 176.08304, 151.07527
11.55-13.53	VBG-diLA	C ₂₄ H ₃₀ O ₁₀	[M+Na ⁺]	501.17288/501.17367	1.58	176.08316, 299.12741, 268.10922

Table S7. Semi-quantitative ^1H - ^{13}C HSQC NMR structural characterisation of *Miscanthus* DES lignin (R9) fractions following sequential solvent fractionation. Note that the DES lignin precipitate (R9) ‘input’ for this experiment originated from a different batch. This batch was obtained by using a steeper heating gradient of the Parr reactor, which resulted in a temperature overshoot (briefly to about 130 °C), and hence suffered from slightly more severe process conditions. Indeed, this more severe processing led to a more impacted overall structure (e.g. lower β -O-4 aryl ether content).

	DES lignin R9 'Input'	EtOAc	EtOH	MeOH	Residue
Yield (% w/w)	-	22.4	28.3	14.9	33.6
Lignin subunits (%)^a					
H (+...)	3.0	7.3	5.1	4.0	4.7
G	54.7	51.0	52.5	57.5	60.0
G _{ox}	0.8	1.0	1.2	1.1	0.0
S	40.4	39.0	40.0	37.0	35.3
S _{ox}	1.1	1.8	1.1	0.4	0.0
S/G	0.75	0.78	0.77	0.64	0.59
Hydroxycinnamates (per 100 ar)^b					
<i>p</i> -coumarate	21.1	17.2	21.5	20.5	33.7
ferulate	3.4	3.6	3.6	4.4	0.0
Interunit linkages (per 100 ar)^b					
β -O-4 aryl ether G+H	5.6	3.7	6.3	7.4	4.4
β -O-4 aryl ether S	0.0	0.0	0.0	0.0	0.0
β -O-4 aryl ether substituted	18.6	10.8	18.5	20.0	9.7
total β -O-4 aryl ethers	24.2	14.5	24.8	27.4	14.1
β -5 phenylcoumaran	3.8	4.3	4.0	3.2	2.8
β - β resinol	0.5	0.3	0.3	0.8	0.0
β - β tetrahydrofuran acylated	0.4	0.2	0.7	0.1	0.0
total	29.0	19.3	29.8	31.6	16.9
End-units (per 100 ar)^b					
benzaldehyde	0.1	0.5	0.0	0.0	0.0
Hibbert ketone	3.4	2.0	2.5	4.0	3.9
DES incorporation (per 100 ar)^b					
lactic acid	22.1	18.3	16.9	17.6	27.3
choline	2.4	0.0	2.2	4.4	7.2

^a relative distribution of lignin subunits (H+G+G_{ox}+S+S_{ox} =100)

^b relative volume integral of substructure versus volume integral of total lignin subunits

Table S8. Semi-quantitative ^1H - ^{13}C HSQC NMR structural characterisation of *Miscanthus*, *Eucalyptus* and pine DES lignins obtained at three pulping temperatures for 1 h.

	<i>Miscanthus</i>			<i>Eucalyptus</i>			Pine		
	120 °C	140 °C	160 °C	120 °C	140 °C	160 °C	120 °C	140 °C	160 °C
Lignin subunits (%)^a									
G	56.6	53.1	55.9	29.6	28.5	37.1	100	97.4	98.7
G_{ox}	0.7	1.0	1.5	1.8	1.8	0.0	0.0	2.6	1.3
S	41.4	44.3	40.4	64.3	65.0	59.9	0.0	0.0	0.0
S_{ox}	1.3	1.6	2.2	4.3	4.8	3.0	0.0	0.0	0.0
S/G	0.74	0.85	0.74	2.18	2.31	1.69	-	-	
Hydroxycinnamates (per 100 ar)^b									
<i>p</i>-coumarate	30.5	24.8	14.5	0.0	0.0	0.0	0.0	0.0	0.0
ferulate	5.5	4.6	1.9	0.0	0.0	0.0	0.0	0.0	0.0
Interunit linkages (per 100 ar)^b									
β-O-4 aryl ether G+H	14.5	6.6	0.7	14.6	5.0	0.0	5.1	1.7	0.0
β-O-4 aryl ether S	4.3	0.0	0.0	11.2	1.0	0.0	0.0	0.0	0.0
β-O-4 aryl ether substituted^c	27.5	18.7	4.5	16.5	8.3	1.2	24.4	14.4	4.4
total β-O-4 aryl ethers	46.3	25.3	5.2	42.3	14.3	1.2	29.4	16.1	4.4
β-5 phenylcoumaran	6.1	3.9	2.4	2.1	0.8	0.0	9.2	6.8	2.1
β-β resinol	1.0	0.5	0.4	4.5	3.1	1.5	1.9	1.7	0.9
β-β tetrahydrofuran acylated	2.3	0.6	0.1	0.0	0.0	0.0	0.0	0.0	0.0
total	55.6	30.3	8.0	49.0	18.2	2.7	40.5	24.6	7.4
End-units (per 100 ar)^b									
cinnamaldehyde	0.0	0.0	0.0	0.0	0.0	0.0	3.1	2.3	0.7
benzaldehyde	2.0	1.4	0.0	1.2	0.9	0.0	0.1	0.0	0.0
Hibbert ketone	2.1	3.0	4.4	0.9	2.5	2.1	3.1	4.4	0.0
DES incorporation (per 100 ar)^b									
lactic acid	12.7	18.2	17.1	12.9	14.3	12.4	14.5	18.8	17.5
choline	2.7	2.9	1.0	1.3	1.3	0.0	0.7	1.3	0.0

^a relative distribution of lignin subunits ($\text{H}+\text{G}+\text{G}_{\text{ox}}+\text{S}+\text{S}_{\text{ox}}=100$)

^b relative volume integral of substructure versus volume integral of total lignin subunits

^c given the potential overlap of $\text{C}_{\alpha}\text{-H}_{\alpha}$ and $\text{C}_{\beta}\text{-H}_{\beta}$ correlations semi-quantified values might be overestimated

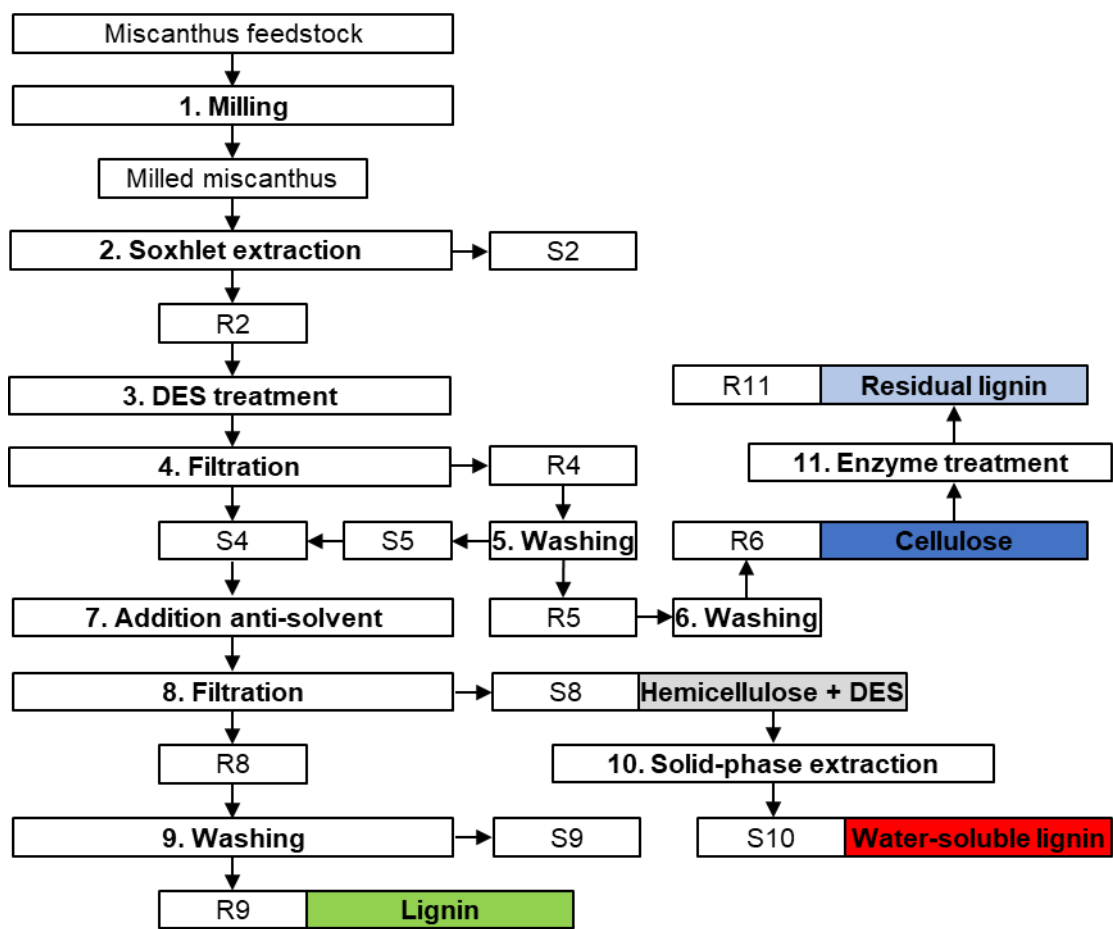


Figure S1. DES fractionation scheme of *Miscanthus* biomass. R: insoluble residue, S: soluble fraction.

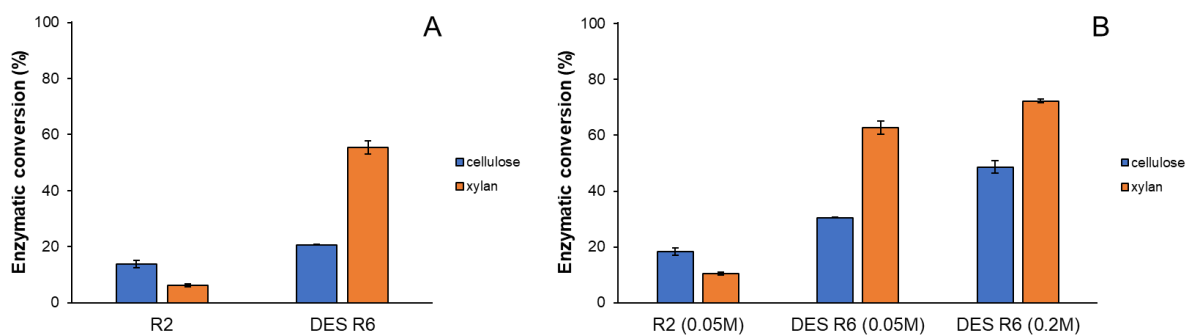
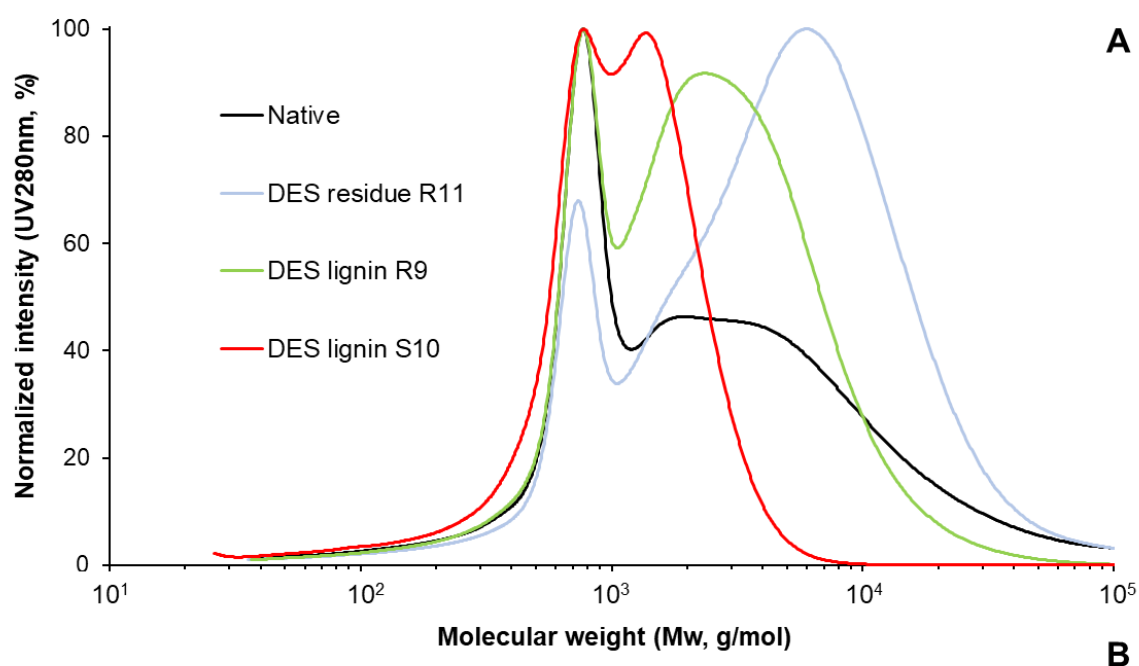


Figure S2. Enzymatic carbohydrate conversion of untreated *Miscanthus* (R2) and the pulp residue following DES pulping (R6) (A) and after mild saponification (B), with alkali strength used in brackets. Average and standard deviation of duplicates.



	Total elution profile			Excluding saponifiable fraction		
	M_w (g/mol)	M_n (g/mol)	\bar{D} (M_w/M_n)	M_w (g/mol)	M_n (g/mol)	\bar{D} (M_w/M_n)
native	8050	650	12.4	12990	256	5.1
DES residue R11	9250	1090	8.5	11220	3170	3.5
DES lignin R9	3540	740	4.8	4810	1940	2.5
DES lignin S10	900	460	2.0	1380	1060	1.3

Figure S3. Alkaline SEC elution profiles of *Miscanthus* lignin fractions (A) and molecular weight distributions based on total elution profiles and excluding the saponifiable fraction (B).

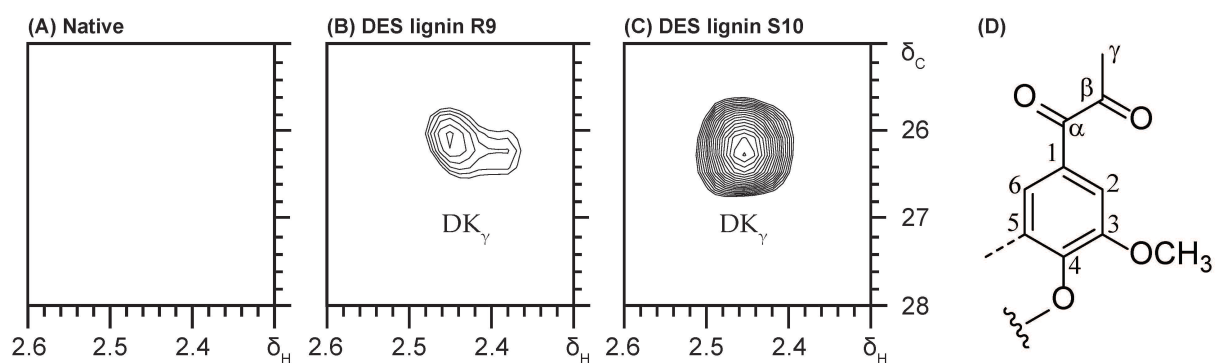


Figure S4. Selected regions of HSQC spectra (400 MHz, DMSO- d_6) of native *Miscanthus* lignin, DES lignin R9 and DES lignin S10 and annotated diketone substructure.

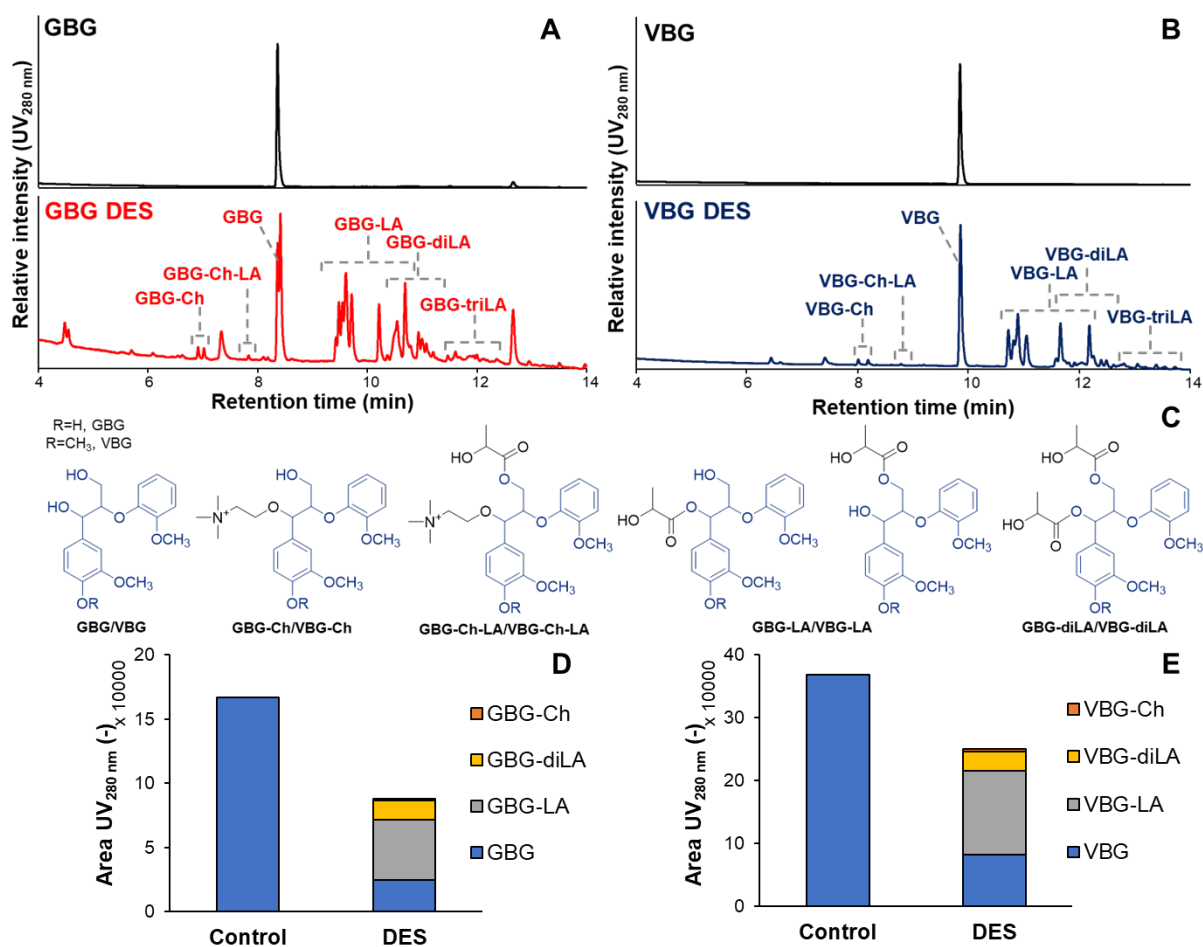


Figure S5. UHPLC-PDA-HR-MS chromatograms of GBG (A) and VBG (B) before and after DES pulping, annotated substructures (C) and semi-quantification based on UV_{280nm} absorbance (D, E). Note that the work-up strategy for these samples was different as compared to GBG/SBG conversion in Figure 2 of the main manuscript, as described in the experimental section.

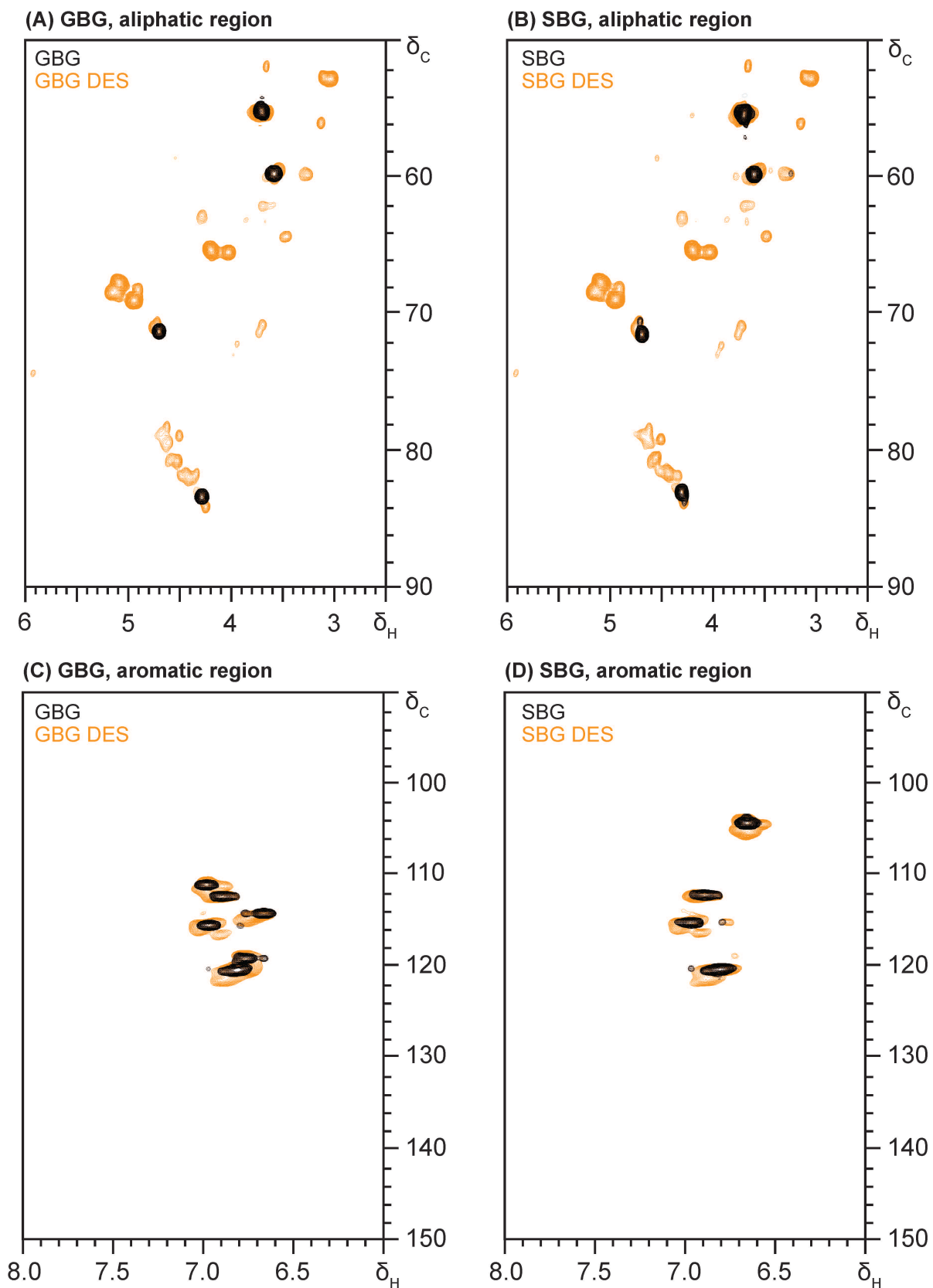


Figure S6. Overlay of aliphatic and aromatic regions of HSQC spectra (400 MHz, DMSO-d₆) of the GBG (A, C) and SBG (B, D) before (black) and after (orange) DES reaction.

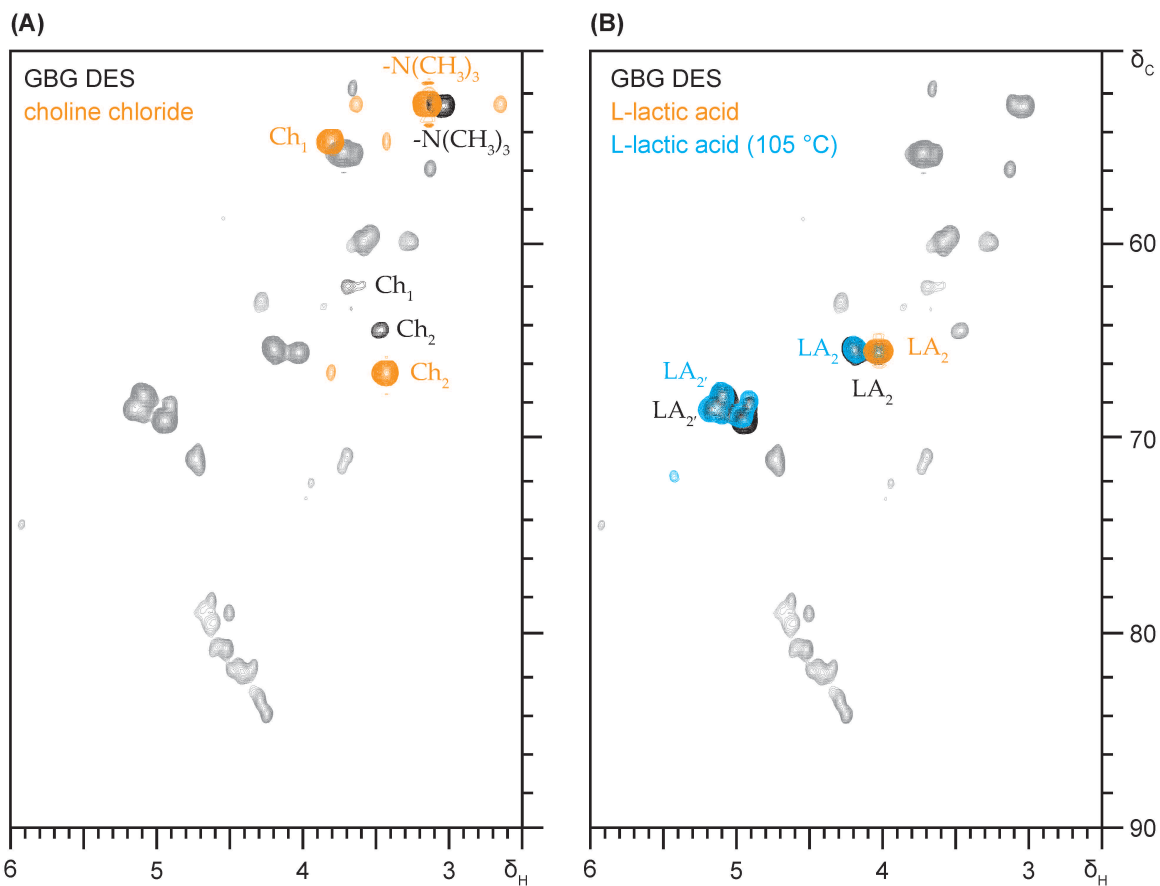


Figure S7. Overlay of HSQC spectra (400 MHz, DMSO- d_6) of GBG DES with choline chloride (A) and lactic acid, before and after heating at 105°C for 24 h (B).

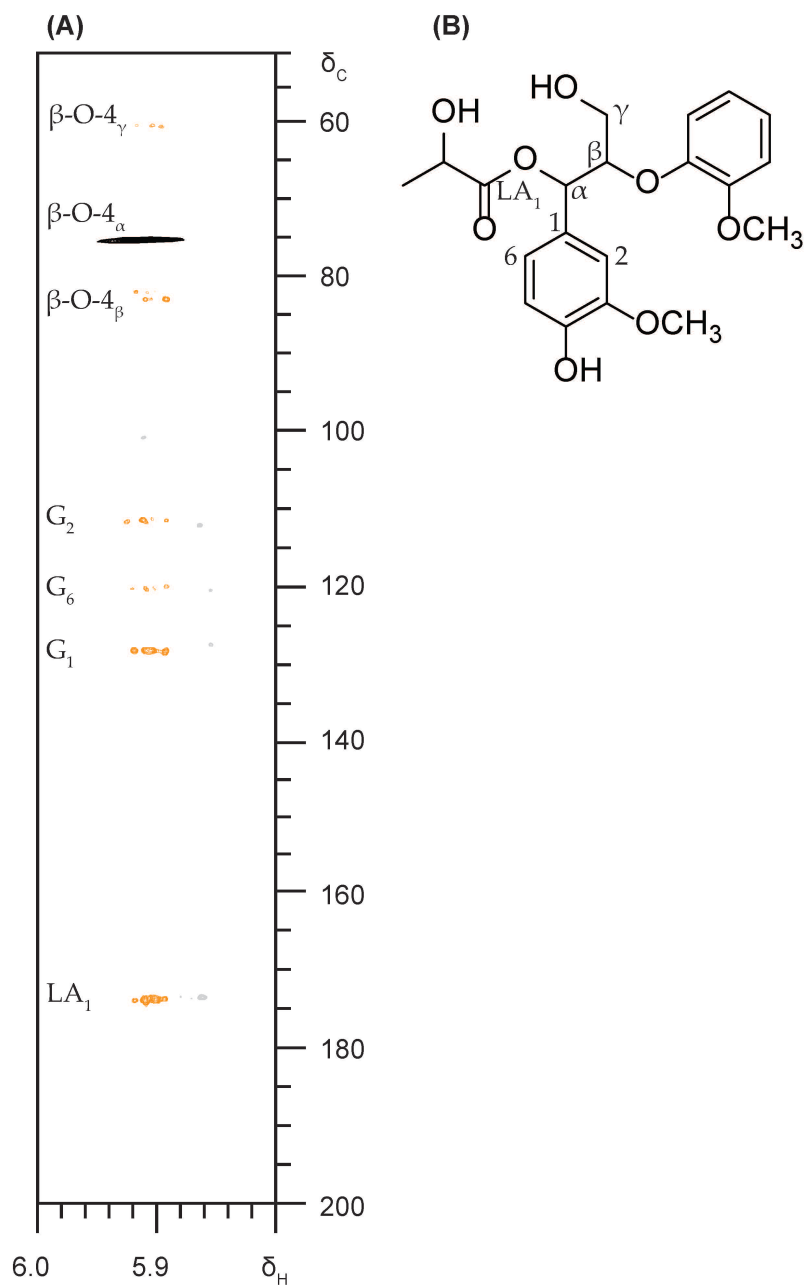


Figure S8. Overlay of HSQC (black) and HMBC (orange) spectra of GBG DES (600 MHz, DMSO- d_6) (A) and annotated α -esterified lactic acid substructure (B).

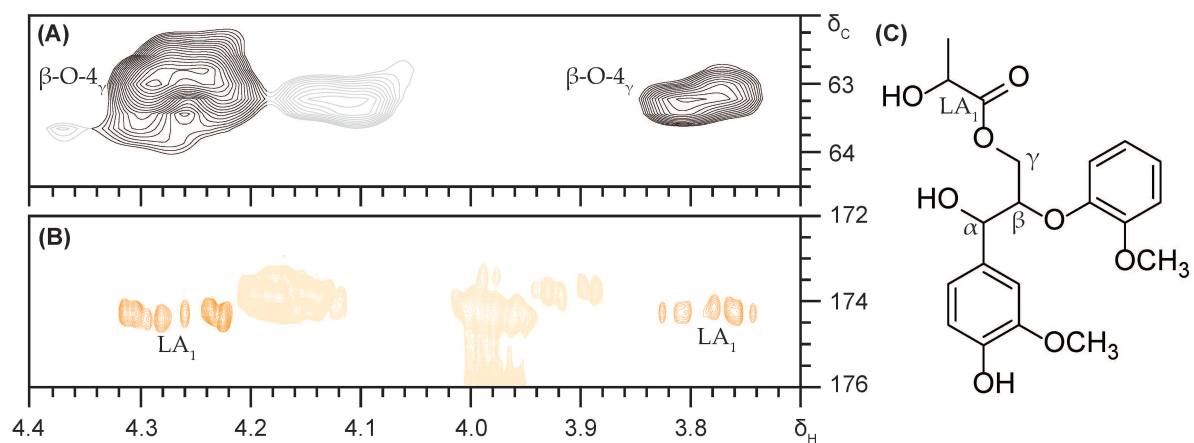


Figure S9. Selected regions of HSQC (A) and HMBC (B) spectra of GBG DES (600 MHz, DMSO-d₆) and annotation of γ -esterified lactic acid substructure (C).

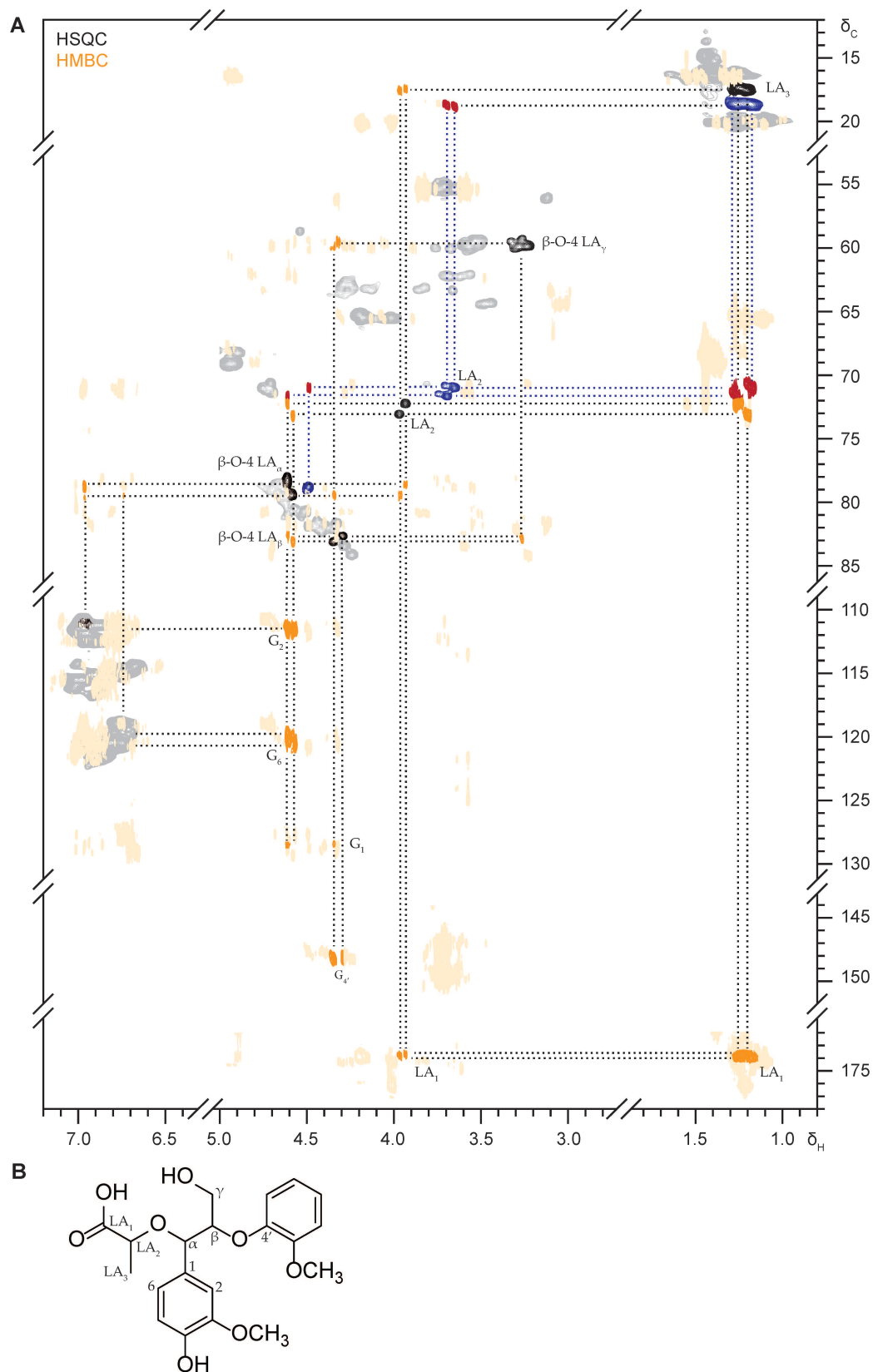


Figure S10. Two-dimensional NMR analysis (600 MHz, DMSO- d_6) of GBG after DES reaction. Overlaid HSQC and HMBC NMR spectra (A) with annotated HSQC signals in black and unannotated in grey, annotated HMBC signals in orange and unannotated in light orange. Structure of benzylic lactate etherified GBG with annotations (B). HSQC (blue) and HMBC (red) also belong to a benzylic lactate etherified substructure, though the exact structural motif could not be elucidated.

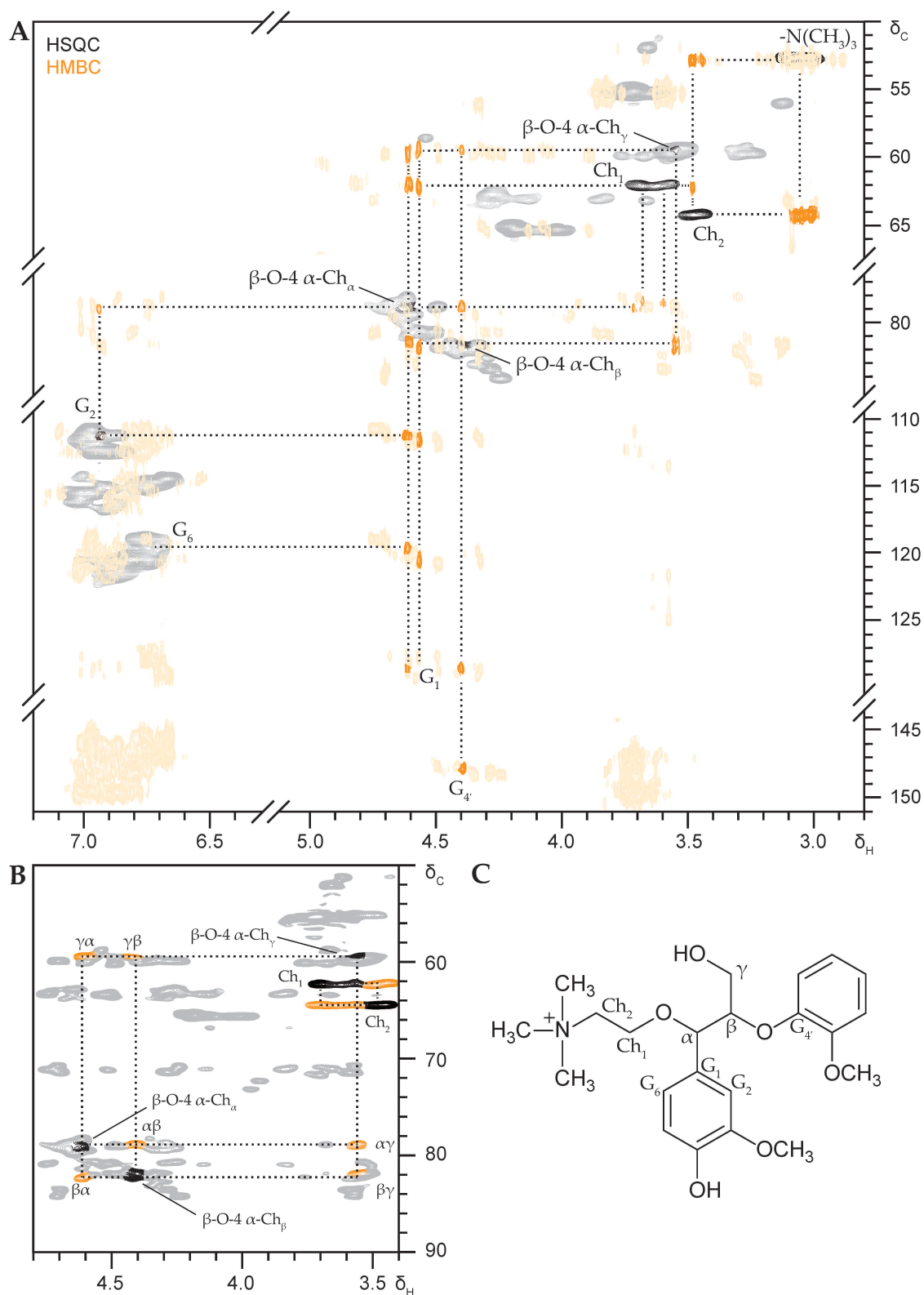


Figure S11. Two-dimensional NMR analysis (600 MHz, DMSO- d_6) of GBG after DES reaction. Overlaid HSQC and HMBC NMR spectra (A) with annotated HSQC signals in black and unannotated in grey, annotated HMBC signals in orange and unannotated in light orange; HSQC-TOCSY NMR spectrum (B) with annotated HSQC signals in black, TOCSY correlation peaks in orange and unannotated in grey; Structure of benzylic choline etherified GBG with annotations (C).

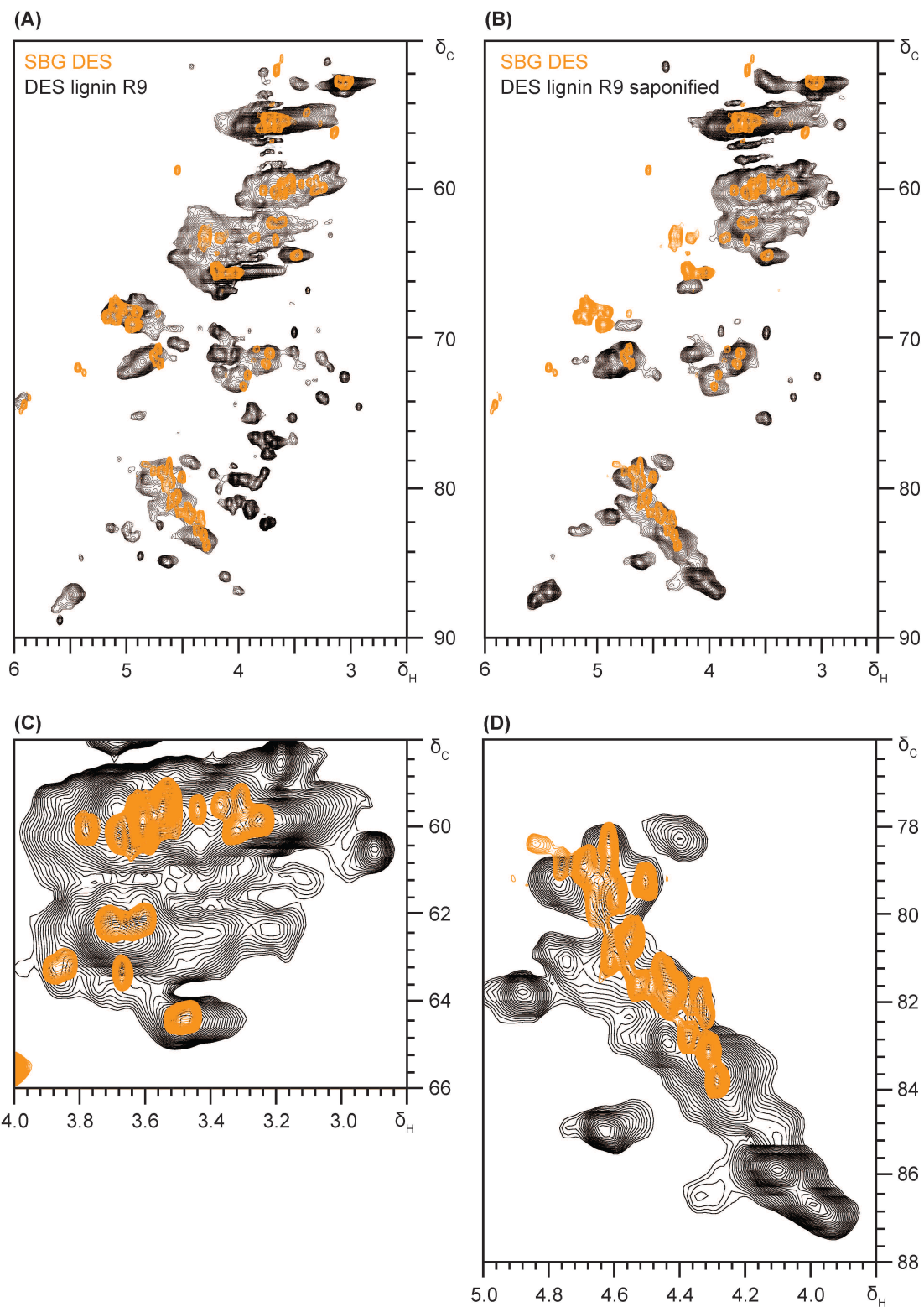


Figure S12. Overlay of selected regions of HSQC NMR spectra (600 MHz, DMSO- d_6) of SBG after DES conversion (orange) and DES Lignin R9 before (black in A) and after saponification (black in B, C, D).

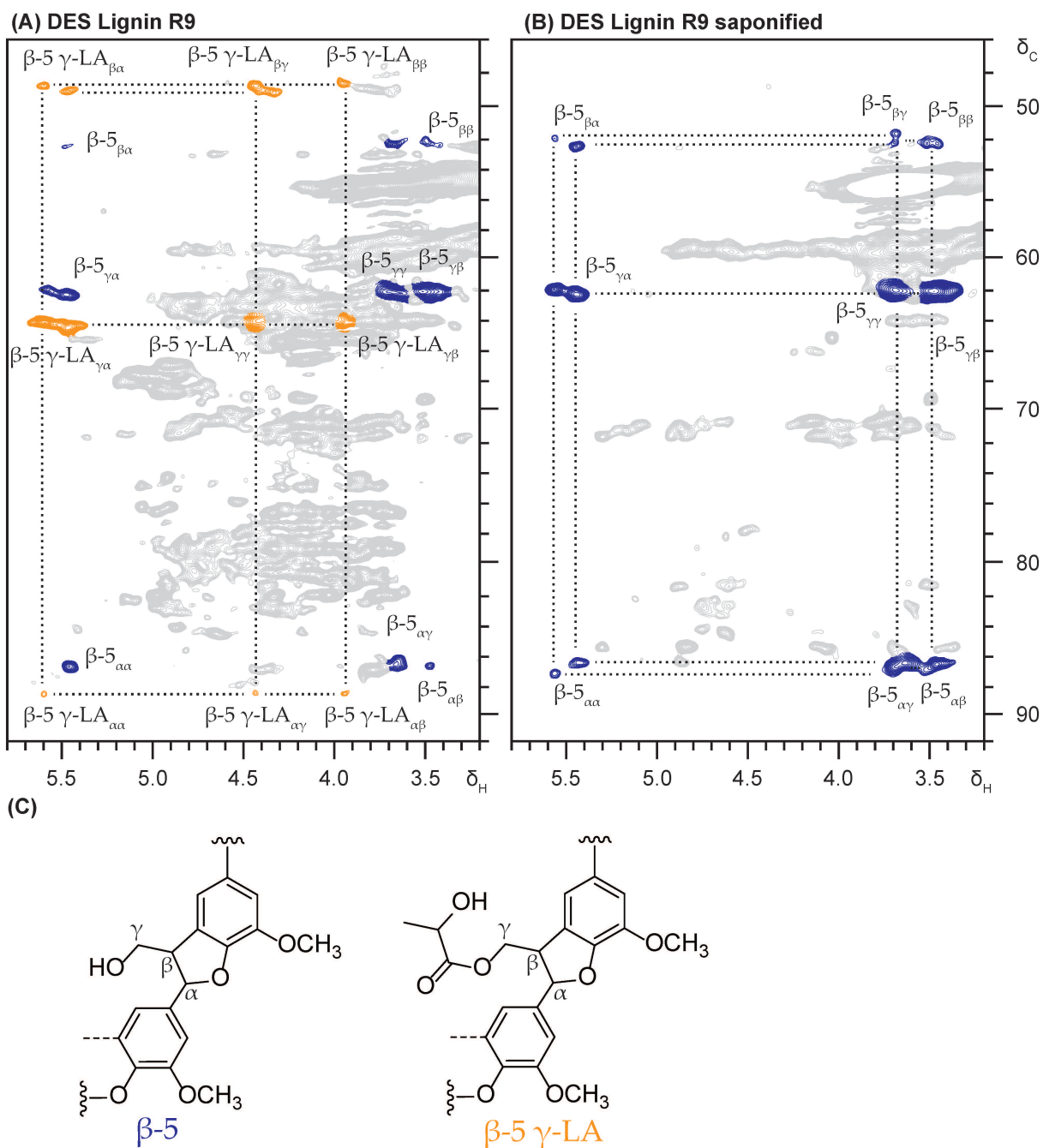
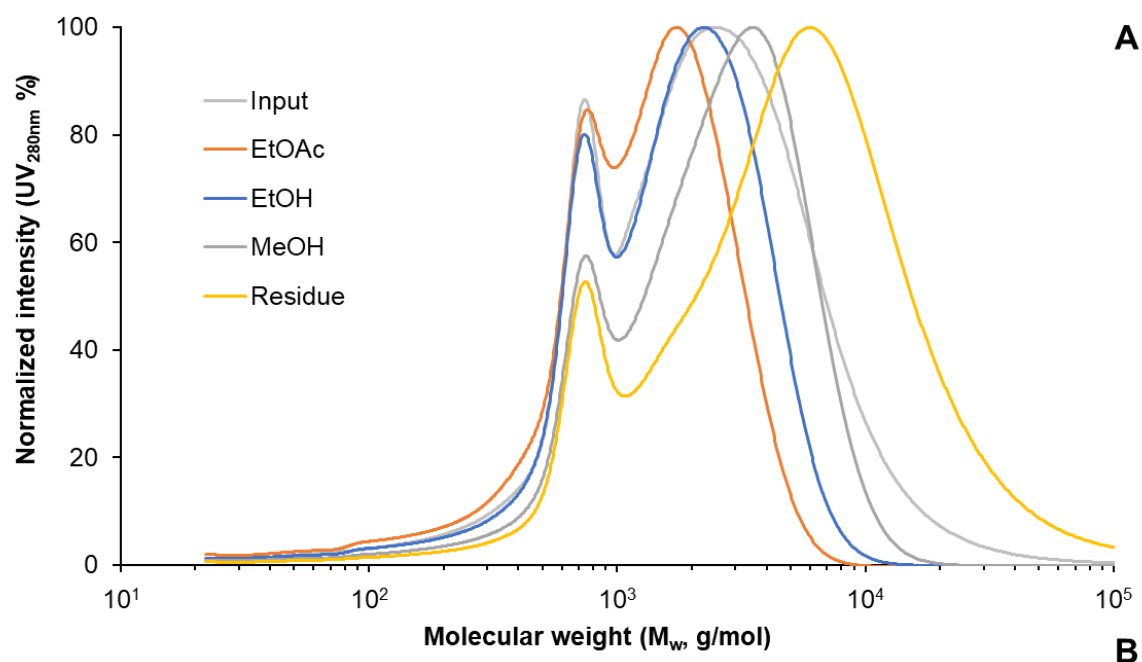


Figure S13. HSQC-TOCSY NMR spectra (600 MHz, DMSO- d_6) of DES Lignin R9 before (A) and after saponification (B). Annotated β -5 (blue) and β -5 γ -LA (orange) substructures in C, not annotated/assigned in grey.



	Total elution profile			Excluding saponifiable fraction		
	M_w (g/mol)	M_n (g/mol)	\bar{D} (M_w/M_n)	M_w (g/mol)	M_n (g/mol)	\bar{D} (M_w/M_n)
DES lignin 'input'	2640	460	5.7	3390	1020	3.3
EtOAc	1220	530	2.3	1740	1260	1.4
EtOH	1730	650	2.7	2320	1530	1.5
MeOH	2850	870	3.3	3530	2000	1.8
Residue	10330	1320	7.8	12220	3510	3.5

Figure S14. Alkaline SEC elution profiles of *Miscanthus* DES lignin fractions following sequential solvent fractionation (A) and molecular weight distributions based on total elution profiles and excluding the saponifiable fraction (B). Note that the DES lignin precipitate (R9) 'input' for this experiment originated from a different batch. This batch was obtained by using a steeper heating gradient of the Parr reactor, which resulted in a temperature overshoot (briefly to about 130 °C), and hence suffered from slightly more severe process conditions. Indeed, this more severe processing led to a slightly lower molecular weight compared to the DES lignin precipitate discussed in the main manuscript (Figure S3) and HSQC NMR correspondingly showed a slightly more impacted overall structure (Table S7).

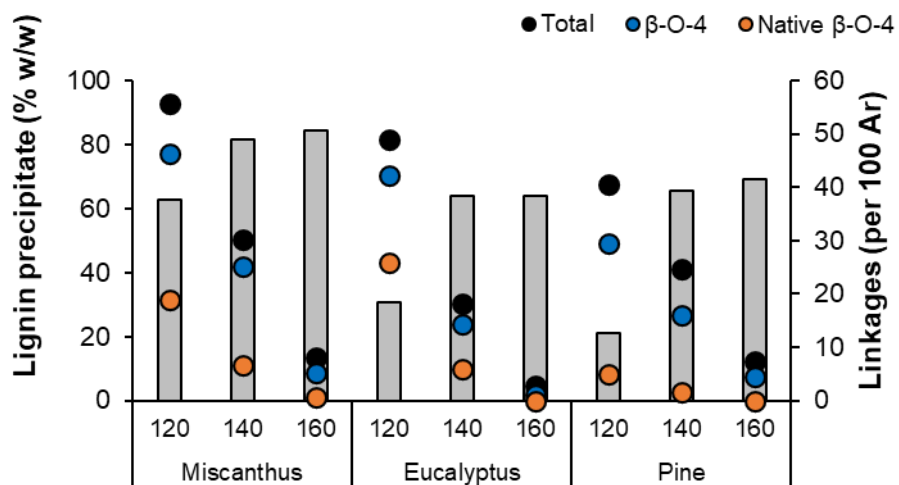


Figure S15. Small scale DES pulping lignin precipitate yields (bars) and interunit linkage content measured by HSQC NMR (circles) for *Miscanthus*, *Eucalyptus* and pine feedstocks at increasing pulping temperatures (°C) for 1 h.

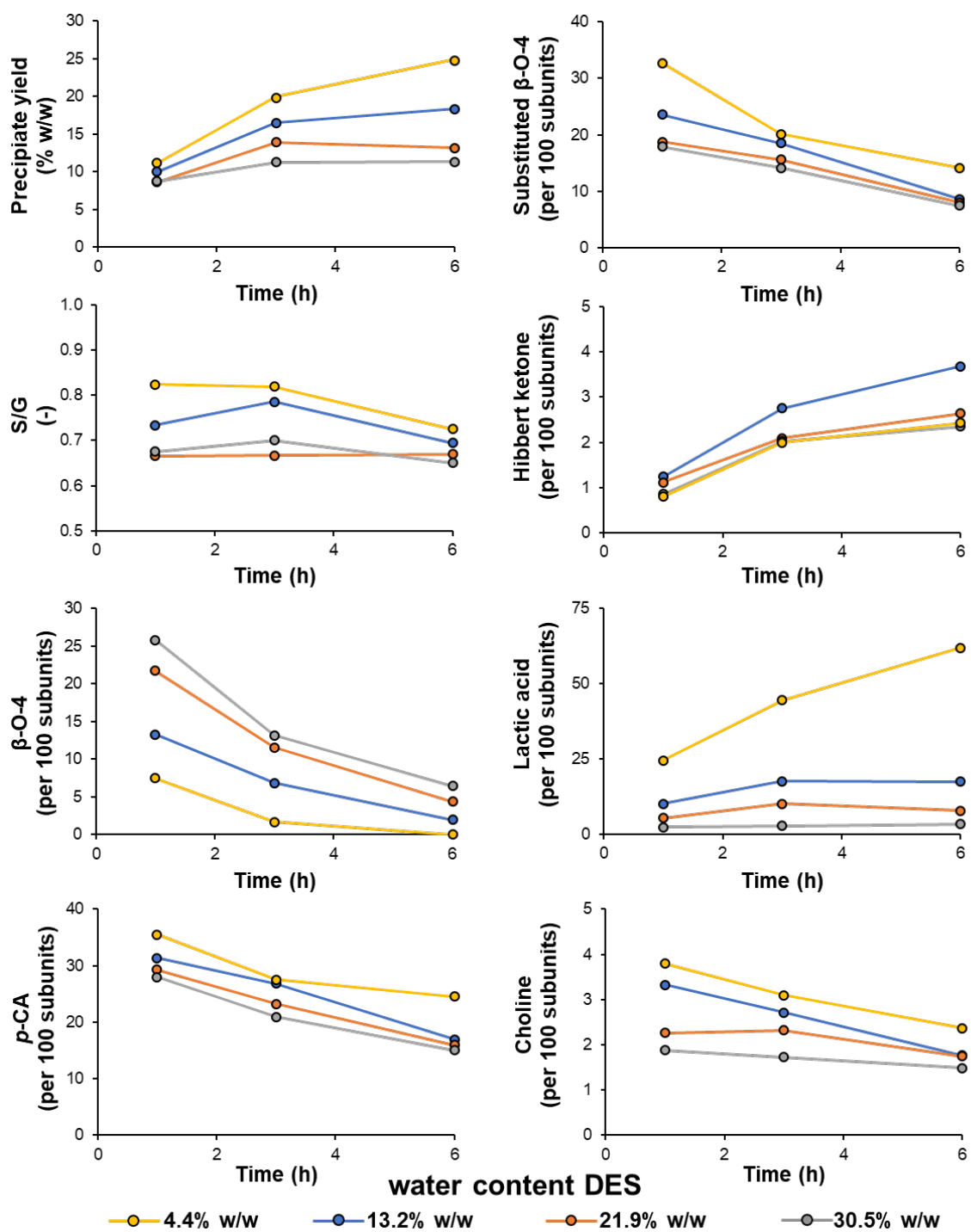


Figure S16. Small scale DES pulping lignin precipitate yields and structural features as determined by HSQC NMR for various DES water contents and reaction durations.

References

1. G. van Erven, N. Nayan, A. S. M. Sonnenberg, W. H. Hendriks, J. W. Cone and M. A. Kabel, *Biotechnol. Biofuels*, 2018, **11**, 1-16.
2. L. Landucci, R. A. Smith, S. Liu, S. D. Karlen and J. Ralph, *Energy Fuels*, 2020, **34**, 16274-16283.
3. G. van Erven, A. F. Kleijn, A. Patyshakuliyeva, M. Di Falco, A. Tsang, R. P. de Vries, W. J. H. van Berkel and M. A. Kabel, *Biotechnol. Biofuels*, 2020, **13**, 1-12.
4. T. M. Mouthier, B. de Rink, G. van Erven, P. de Gijssel, H. A. Schols and M. A. Kabel, *Bioresour. Technol.*, 2019, **272**, 288-299.
5. G. van Erven, P. Hendrickx, M. Al Hassan, B. Beelen, R. op den Kamp, E. Keijsers, K. van der Cruijssen, L. M. Trindade, P. F. H. Harmsen and A. F. van Peer, *ACS Sustainable Chem. Eng.*, 2023, **11**, 6752-6764.
6. N. Blumenkrantz and G. Asboe-Hansen, *Anal. Biochem.*, 1973, **54**, 484-489.
7. G. van Erven, R. de Visser, P. de Waard, W. J. H. van Berkel and M. A. Kabel, *ACS Sustainable Chem. Eng.*, 2019, **7**, 20070-20076.
8. G. van Erven, R. de Visser, D. W. H. Merckx, W. Strolenberg, P. de Gijssel, H. Gruppen and M. A. Kabel, *Anal. Chem.*, 2017, **89**, 10907-10916.
9. J. C. Del Río, J. Rencoret, P. Prinsen, Á. T. Martínez, J. Ralph and A. Gutiérrez, *J. Agric. Food Chem.*, 2012, **60**, 5922-5935.
10. S. A. Ralph, J. Ralph and L. L. Landucci, *Available at URL www.gibrc.org/databases_and_software/nmrdatabase/*, 2009.
11. H. Kim, D. Padmakshan, Y. Li, J. Rencoret, R. D. Hatfield and J. Ralph, *Biomacromolecules*, 2017, **18**, 4184-4195.
12. R. J. A. Gosselink, J. E. G. van Dam, E. de Jong, E. L. Scott, J. P. M. Sanders, J. Li and G. Gellerstedt, *Holzforschung*, 2010, **64**, 193-200.
13. A. Granata and D. S. Argyropoulos, *J. Agric. Food Chem.*, 1995, **43**, 1538-1544.
14. S. Constant, H. L. J. Wienk, A. E. Frissen, P. de Peinder, R. Boelens, D. S. Van Es, R. J. H. Grisel, B. M. Weckhuysen, W. J. J. Huijgen and R. J. A. Gosselink, *Green Chem.*, 2016, **18**, 2651-2665.
15. E. S. Morais, A. M. Da Costa Lopes, M. G. Freire, C. S. Freire and A. J. Silvestre, *ChemSusChem*, 2021, **14**, 686-698.
16. G. Zeng, L. Zhang, B. Qi, J. Luo and Y. Wan, *Bioresour. Technol.*, 2023, **380**, 129085.
17. G. van Erven, R. Hilgers, P. d. Waard, E.-J. Gladbeek, W. J. H. van Berkel and M. A. Kabel, *ACS Sustainable Chem. Eng.*, 2019, **7**, 16757-16764.